

Effect of circularly polarized light on germination, hypocotyl elongation and biomass production of arabidopsis and lettuce: Involvement of phytochrome B

Enkhsukh Lkhamkhuu¹, Kazunori Zikihara^{2,a}, Hitomi Katsura²,
Satoru Tokutomi^{2,3,**}, Takafumi Hosokawa⁴, Yoshihisa Usami⁴,
Mitsuyoshi Ichihashi⁴, Junji Yamaguchi⁵, Kenji Monde^{1,*}

¹ Graduate School of Life Science, Faculty of Advanced Life Science, Hokkaido University, Sapporo 001-0021, Japan;

² Department of Biological Science, Graduate School of Science, Osaka Prefecture University, Sakai, Osaka 599-8531,

Japan; ³ Botanical Gardens, Tohoku University, Sendai, Miyagi 980-0862, Japan; ⁴ Research and Development Management Headquarters, Fuji Film Corporation, Kanagawa 258-8577, Japan; ⁵ Faculty of Science, Hokkaido University, Sapporo 060-0810, Japan

* E-mail: kmonde@sci.hokudai.ac.jp Tel: +81-11-706-9041 Fax: +81-11-706-9540

** E-mail: toxan@b.s.osakafu-u.ac.jp Tel: +81-22-795-6765 Fax: +81-22-795-6766

Received December 3, 2019; accepted December 19, 2019 (Edited by Y.Chiba)

Abstract Circular dichroism (CD), defined as the differential absorption of left- and right-handed circularly polarized light (CPL), is a useful spectroscopic technique for structural studies of biological systems composed of chiral molecules. The present study evaluated the effects of CPL on germination, hypocotyl elongation and biomass production of Arabidopsis and lettuce. Higher germination rates were observed when Arabidopsis and lettuce seedlings were irradiated with red right-handed CPL (R-CPL) than with red left-handed CPL (L-CPL). Hypocotyl elongation was effectively inhibited when Arabidopsis and lettuce seedlings were irradiated with red R-CPL than with red L-CPL. This difference was not observed when a phytochrome B (phyB) deficient mutant of Arabidopsis was irradiated, suggesting that inhibition of elongation by red R-CPL was mediated by phyB. White R-CPL induced greater biomass production by adult Arabidopsis plants, as determined by their fresh shoot weight, than white L-CPL. To determine the molecular basis of these CPL effects, CD spectra and the effect of CPL on the photoreaction of a sensory module of Arabidopsis phyB were measured. The red light-absorbing form of phyB showed a negative CD in the red light-absorbing region, consistent with the results of germination, inhibition of hypocotyl elongation and biomass production. L-CPL and R-CPL, however, did not differ in their ability to induce the interconversion of the red light-absorbing and far-red light-absorbing forms of phyB. These findings suggest that these CPL effects involve phyB, along with other photoreceptors and the photosynthetic process.

Key words: circularly polarized light, germination, hypocotyl elongation, photoreaction, phytochrome.

Introduction

Light, especially sunlight, is a fundamental energy source. Plants utilize sunlight to synthesize carbohydrates through the process of photosynthesis. Most natural light is unpolarized, as it consists of mixtures of randomly polarized light, whereas polarized light, such as linearly polarized light (LPL) and circularly polarized light (CPL) can be generated artificially by polarizers. Polarized light is useful for spectroscopic studies analyzing the

structure of chiral materials (Li et al. 2015). The plane of LPL is rotated to the left or right by passing through chiral materials, such as amino acids and carbohydrates, depending on their chirality, also known as optical activity (Bromage et al. 2003). The differential absorption of left- (L-CPL) and right- (R-CPL) CPL is defined as circular dichroism (CD) (Polavarapu 2002). These spectroscopic features provide essential information to determine the stereochemical structures of these compounds, including their absolute configurations,

Abbreviations: *At*, *Arabidopsis thaliana*; CD, circular dichroism; CPL, circular polarized light; cry, cryptochrome; FMN, flavin mononucleotide; LOV, light, oxygen, voltage-sensing domain; LPL, linearly polarized light; L-CPL, left-handed circular polarized light; PCB, phycocyanobilin; Pfr, far-red light-absorbing form; phot, phototropin; phy, phytochrome; phyA, phytochrome A; phyB, phytochrome B; Pr, red light-absorbing form; PΦB, phytochromobilin; R-CPL, right-handed circular polarized light; UV, ultraviolet; Vis, visible.

^a Present address: Research & Development Center for Cell Therapy, Foundation for Biomedical Research and Innovation at Kobe, Kobe 650-0047, Japan

This article can be found at <http://www.jspcmb.jp/>

Published online March 20, 2020

which are difficult to determine by other methods.

To date, most chiroptical spectroscopic studies have been performed at the molecular level (Harada et al. 2012; Tranter 2016). Many biopolymers in organisms contain optically active molecules, such as L-amino acids and D-glucose, which absorb L-CPL and R-CPL unequally. CD is an established spectroscopic method used to analyze the secondary structure of proteins (Whitmore and Wallace 2008) and DNA (Vorlíčková et al. 2012). Furthermore, complexes of biopolymers, such as arthropod cuticles, plant cell walls and human compact bone osteon, form cholesteric liquid crystals and scatter CPL (Mitov and Dessaud 2006). Studies have suggested that communications in the scarab beetle *Chrysina gloriosa* involve CPL reflection (Brady and Cummings 2010), and several types of crustaceans, including stomatopods (Chiou et al. 2008), sapphirinidae copepods (Baar et al. 2014) and mantis shrimp (Gagnon et al. 2015), have been reported to recognize CPL. Plant tissues that reflect CPL include *Polia* fruit (Vignolini et al. 2012), leaves of the herb *Mapania caudate* (Strout et al. 2013) and starch granules from *Solanum tuberosum* (Zhuo et al. 2014). CPL reflection has also been used to analyze the fibrillar structure of bone (Spiesz et al. 2011).

In plants, granal chloroplasts show CD in a red light-absorbing region of chlorophyll (Gregory and Raps 1974), with circularly polarized chlorophyll luminescence used to measure chiral macroaggregates of light-harvesting chlorophyll–protein complexes in chloroplasts (Hall et al. 2016; Patty et al. 2018). CPL was also shown to have net photosynthetic activity and to be involved in the synthesis of chlorophyll in the unicellular marine flagellate, *Dunaliella euchlora*. R-CPL showed greater activity than L-CPL, suggesting that the receptor pigments responsible for these phenomena sense CD (McLeod 1957). To date, however, only one study has reported that CPL had a differential effect on plant growth. In that study, L-CPL induced faster growth of the shoots of lentil and pea plants than R-CPL although the CPL did not change significantly after penetration through the outer layer cells of leaves and stems (Shibayev and Pergolizzi 2011). Thus, the effect of CPL on plant growth is poorly understood.

In addition to photosynthesis, physiological responses of plants to light are regulated by photoreceptors. Immobile, photosynthetic plants must adapt precisely to their environmental conditions, including light. Plants have various photoreceptors that receive light signals over a wide spectrum, ranging far-red to ultraviolet B light (Paik and Huq 2019). These receptors include phytochrome; two blue light receptors, cryptochrome (cry) and phototropin (phot); and UV-B resistance 8 (UVR8).

Phytochrome B (phyB) is a photochromic receptor interconvertible between its red light-absorbing form

(Pr) and its far-red light-absorbing form (Pfr) following exposure to red and far-red light, respectively (Li et al. 2011). Phytochrome B (phyB) has been reported to regulate the germination (Shinomura et al. 1996) and hypocotyl elongation (Reed et al. 1993) of *Arabidopsis*, suggesting that differences in the responses of these plants to R- and L-CPL may be due to the chiral structure of phyB and its different photoreaction to R- and L-CPL. The present study evaluated the effects of CPL on the growth of *Arabidopsis* and lettuce plants, including effects on germination, hypocotyl elongation and biomass production. To determine the molecular basis of CPL perception, the CD spectrum and the effect of CPL on photoconversion were measured with the sensory module of *Arabidopsis* phyB, which binds phycocyanobilin (PCB) rather than the native chromophore phytochromobilin (PΦB). These findings showed that phyB, along with other photoreceptors and photosynthesis is involved in the effects of CPL on plant physiological responses.

Materials and methods

Plant materials

Seeds of *Arabidopsis* (*Arabidopsis thaliana*: At) wild type (ecotype Columbia-0) and its phyB deficient mutant (*phyB*) were the kind gifts of Prof. Akira Nagatani at Kyoto University. Lettuce seeds (*Lactuca sativa* L.) were purchased from Sakata Seed Corporation (Yokohama, Japan). Surface-sterilized seeds were placed on filter paper soaked with water or Murashige and Skoog (MS) medium supplemented with 2% (W/V) sucrose (Germination Inducible Medium: GIM) in a Petri dish. The seeds were incubated in the dark at 4°C for 48 h to synchronize germination. The detailed growth conditions are shown in each section.

Light condition in growth chamber

Plants were cultured in LED plant growth chambers (LH-70LED-DT, Nippon Medical & Chemical Instruments Co., Ltd., Japan), containing three monochromatic LEDs (red LED, λ_{max} =660 nm; green LED, λ_{max} =525 nm; and blue, LED λ_{max} =450 nm). CPL was generated by filtering the LED light through circularly polarizing filters (Polarization Control Film, Fujifilm Corporation, Japan). Each filter consisted of a linear polarization plate and a quarter wavelength plate. The chiroptical purity of L- and R-CPL was examined by a Haze meter (NDH2000, Nippon Denshoku Industries Co., LTD., Japan) (Supplementary Figure S4); negligible differences in intensity and purity were observed between L- and R-CPL. The inner walls of the chamber were covered with black paper to avoid reflection of light. In this study, the term “white light” indicates the mixture of red, green and blue light supplied by the three LEDs in the growth chamber. Monochromatic light was generated by turning on only the red, green or blue LED. The humidity of the chamber was set at 50%.

Germination assay

Arabidopsis seeds (60–200 grains) were placed on water-soaked filter paper in Petri dishes. After incubation at 4°C for 48 h in the dark, the seeds were irradiated with red L- or R-CPL ($1.02 \mu\text{mol}/\text{m}^2/\text{s}$) for 10 min at 22°C and kept in the dark for 3 days at 22°C. Lettuce seeds were treated similarly, except that the intensity of irradiated light was $0.36 \mu\text{mol}/\text{m}^2/\text{s}$. Germinated seeds were counted, and germination rates were calculated and compared by Student's *t*-tests.

Hypocotyl elongation assay

Germinated wild type (Ler-0) and *phyB* mutant Arabidopsis seeds (20 grains) on water-soaked filter paper in Petri dishes were irradiated with unpolarized white light ($10.87 \mu\text{mol}/\text{m}^2/\text{s}$) for 8 h at 22°C. The seeds were cultured under continuous red L- or R-CPL ($1.02 \mu\text{mol}/\text{m}^2/\text{s}$) irradiation for 7 or 10 days at 22°C, and the shoots were harvested. Germinated lettuce seeds (20 grains) were cultured and the shoots harvested using the same protocol, except for the omission of white light irradiation. Harvested shoots were photographed, and their hypocotyl lengths were quantified using ImageJ computer software (<https://imagej.nih.gov/ij/download.html>) and compared by Student's *t*-tests.

Biomass assay

Approximately 12 Arabidopsis seeds germinated on GIM-soaked filter paper in Petri dishes were planted in vermiculite soil in a plastic box (40 mm × 33 mm × 15 mm). The plants were grown under unpolarized white light ($22 \mu\text{mol}/\text{m}^2/\text{s}$) with a 16 h light/8 h dark cycle for 2 weeks in a cultivation room set at 22°C and ca. 50% humidity. Seedlings with leaves of similar size were selected, transferred to the growth chamber, and cultured under white L-CPL or R-CPL ($10.8 \mu\text{mol}/\text{m}^2/\text{s}$) with a 16 h light/8 h dark cycle for 2 weeks at 22°C. The effect of light quality was measured by turning on one of the LEDs (red, green or blue) in the growth chamber during CPL illumination. Because the fluence rates of the red, green, and blue LED illuminators differed, being $29.7 \mu\text{mol}/\text{m}^2/\text{s}$, $5.0 \mu\text{mol}/\text{m}^2/\text{s}$ and $2.3 \mu\text{mol}/\text{m}^2/\text{s}$, respectively, the culture periods were varied, 3 weeks for irradiation with the red and blue LEDs, and 4 weeks for irradiation with the green LED. The total fluences for the red, green and blue CPL cultures were 35.6, 8.1 and 2.8 mol photons, respectively. The shoots were subsequently harvested and weighed. Biomass was quantified as the average fresh weight per above-ground part of an adult plant and compared by Student's *t*-tests.

Preparation of PCB-bound AtphyB-N651

The PCB-bound N-terminal (amino acids 1–651) sensory module of *Arabidopsis thaliana* phyB (AtphyB-N651) was prepared using an *Escherichia coli* (*E. coli*) expression system, essentially as described (Mukougawa et al. 2006). Briefly, AtphyB-N651 was overexpressed in *E. coli* BL21 (DE3) cells as fusion proteins with the chitin binding domains (CBD) of the PCB synthesizing enzymes HO1 and PCYA from *Synechocystis*

sp. PCC6803. The plasmids for the expression of PCB synthesis were the kind gift of Prof. Takayuki Kochi at Kyoto University. The expressed AtphyB-N651 fused to CBD was purified by chitin affinity chromatography on a prepacked Chitin Beads column (3 ml bed vol. New England Biolabs) according to the manufacturer's instructions with modifications. The bound protein was washed and self-cleaved by incubating with a cleavage buffer. The eluted sample was purified by ion column chromatography, desalted on a HiTrap Desalting column (GE Healthcare) equilibrated in buffer containing 20 mM Tris-HCl and 0.1 mM Na₂EDTA, pH 7.8, and applied to a Mono Q 5/50 GL column (GE Healthcare) equilibrated in the same buffer. AtphyB-N651 was eluted by stepwise application of 0, 100, 200 and 500 mM NaCl in buffer, and by monitoring absorption at 280 nm. Fractions surrounding the elution peak were collected and concentrated on a spin column (Amicon Ultra Centrifugal filter, Millipore). All procedures were performed at 4°C under dim green safe light. Based on a Coomassie Blue stained SDS- PAGE gel, the purity of the eluted AtphyB-N651 was estimated to be >95%. Binding of PCB was confirmed at almost 100% by measuring A₆₅₀/A₂₈₀ on a UV-Vis absorption spectrophotometer (Figure 4A).

Spectroscopy

UV-Vis absorption spectra of AtphyB-N651 in a 25 mM Tris-HCl, pH 7.8 buffer containing 0.5 mM Na₂EDTA and 125 mM NaCl were recorded at 25°C with a spectrophotometer (model U-3010; Hitachi-Hitec) equipped with a thermostat controller (model 131-0305, Hitachi-Hitec). Samples in the cuvette were illuminated from above at 650 nm for red light and 715 nm for far-red light using an excitation light of a fluorescent spectrophotometer (model RF5300, Shimadzu) guided through a quartz light guide ($\phi=1 \text{ cm} \times 1 \text{ m}$) and a slit width of 10 nm (Supplementary Figure S5). The intensity of illumination was adjusted by varying the distance between the end of the light guide and the surface of the sample solution in the cuvette and was measured with a photometric sensor (LI-210R, LI-COR). The effects of polarized light on the photoreaction between Pr and Pfr and the reverse reaction was monitored by repeat scanning of the absorption spectra from 500 to 800 nm at 25°C. LPL, L-CPL and R-CPL were generated by a combination of a polarizer (VIS-NIR high contrast polarizer #47-603, Edmund Optics) and a 1/4 wavelength plate (Achromatic waveplate #65-919, Edmund Optics) (Supplementary Figure S6). Chiroptical purity and transmittance of the L- or R-CPL were evaluated by a Haze meter (NDH2000, Nippon Denshoku Industries Co., LTD., Japan). No difference between L- and R-CPL was detected (Supplementary Figure S7).

CD spectra in the UV-Vis absorption region (250–800 nm) were measured at 25°C with a spectropolarimeter (J820, JASCO) equipped with an electric temperature-control system under flowing N₂ gas and an optical path of 1 cm. For each measurement, 10 spectra were collected and averaged. Sample spectra were obtained by subtracting the spectrum of the sample buffer. Before each scan, samples in the cuvette

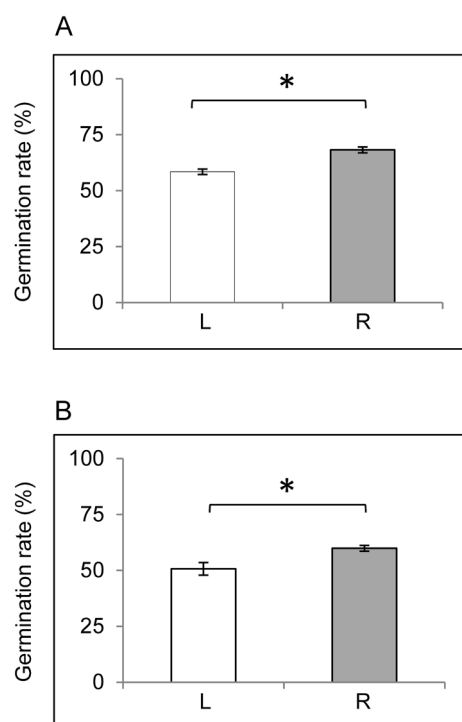


Figure 1. Effect of red CPL on germination of Arabidopsis (A) and lettuce (B) seeds. Cold-treated seeds were irradiated with red L-CPL (L) or R-CPL (R) for 10 min at $1.02 \mu\text{mol}/\text{m}^2/\text{s}$ (A) and $0.36 \mu\text{mol}/\text{m}^2/\text{s}$ (B) at 22°C . After incubation for 3 days in the dark at 22°C , the germinated seeds were counted and germination rates were calculated. * $p < 0.05$ by t -tests, error bar = S.D., $N = 10$.

were irradiated with saturating far-red or red light for 3 min to ensure that *AtphyB-n651* was in a Pfr or a Pr-induced photostationary state, respectively, because the measuring light of the spectropolarimeter has an actinic effect on the UV-visible absorption spectra of the *AtphyB-N651* solutions. To determine the amounts of Pr and Pfr generated by the measuring light of CD, UV-Vis absorption spectra were obtained immediately after the CD measurements. Red and far-red light were supplied from the side of the sample cuvette by the LED illuminators ISL-150X150-H4FRFR (CCS) and ISL-150X150-H4FRFR (CCS), respectively. Irradiated samples were placed in the sample holder of the spectropolarimeter, and CD scans were started immediately.

Results

Effect of red CPL on germination of Arabidopsis and lettuce seeds

The germination rates of Arabidopsis seeds in the presence of L- and R-CPL were 58.4% and 68.2%, respectively, indicating that R-CPL was more effective than L-CPL in the red light-absorbing region (Figure 1A). Similarly, the germination rates of lettuce seeds in the presence of L- and R-CPL were 50.7% and 59.9%, respectively (Figure 1B). Calculations showed that the germination rates of Arabidopsis and lettuce were 1.17-

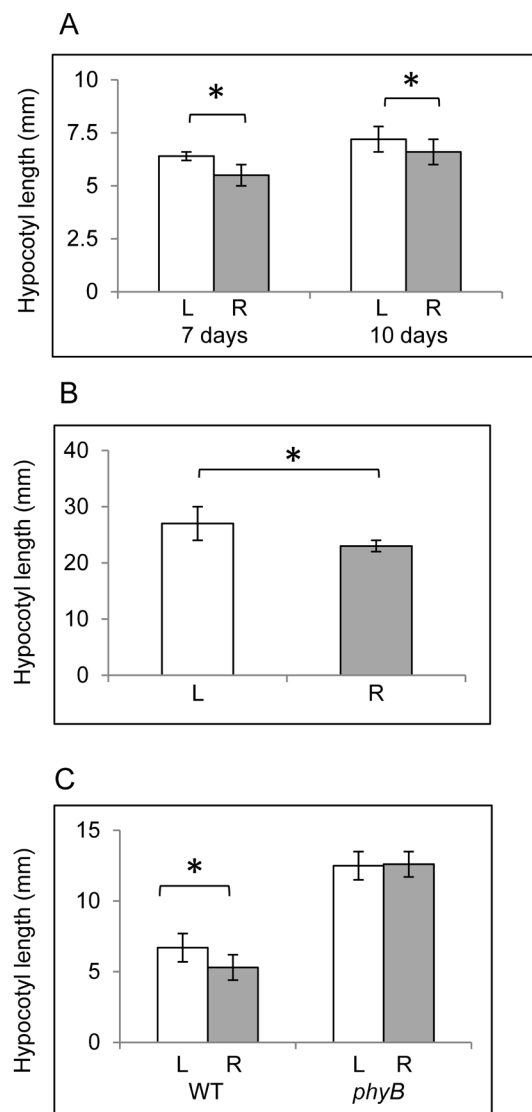


Figure 2. Effect of red CPL on hypocotyl elongation. (A, B) Germinated seeds of Arabidopsis (A) and lettuce (B) were cultured in the growth chamber under continuous red L-CPL (white columns) or R-CPL (grey columns) for 7 or 10 days (A) and 7 days (B) at 22°C . The seedlings were cut and hypocotyl lengths were measured. * $p < 0.05$ by t -tests, error bar = S.D., $N = 5$. (C) Germinated seeds of Arabidopsis wild type (WT) and *phyB* deficient mutant (*phyB*) were cultured in the growth chamber under continuous red L-CPL (white columns) or R-CPL (grey columns) for 7 days at 22°C . The seedlings were cut and hypocotyl lengths were measured. * $p < 0.05$ by t -tests, error bar = S.D., $N = 4$.

and 1.18-fold greater, respectively under R- than L-CPL.

Effect of red CPL on hypocotyl elongation of Arabidopsis and lettuce

Assessment of the effects of red CPL on hypocotyl elongation of Arabidopsis showed that the average hypocotyl lengths under L- and R-CPL were 6.4 mm and 5.4 mm, respectively, for 7-day-old seedlings and 7.2 mm and 6.0 mm, respectively, for 10-day-old seedlings (Figure 2A). Similarly, the average hypocotyl lengths of 7-day-old lettuce seedlings under L- and

R-CPL were 27.2 mm and 23.0 mm, respectively (Figure 2B). Calculations showed that the hypocotyls of 7- and 10-day-old *Arabidopsis* seedlings and of 7-day-old lettuce seedlings were 1.18-, 1.20- and 1.18-fold longer, respectively, under L-CPL than under R-CPL.

Effect of red CPL on hypocotyl elongation of the *phyB*-deficient mutant of *Arabidopsis*

The involvement of *phyB* in the red CPL effect on hypocotyl elongation was assessed by measuring hypocotyl lengths in a *phyB*-deficient mutant of *Arabidopsis* (*phyB*) grown under L-CPL and R-CPL. The average hypocotyl lengths of 7-day-old wild-type seedlings under L-CPL and R-CPL were 6.7 mm and 5.3 mm, similar to the results in Figure 2A. In contrast, hypocotyls of the *phyB* mutant were longer than those of wild-type under both L- and R-CPL, being 12.5 mm and 12.6 mm, respectively, and were almost equal (Figure 2C), suggesting that *phyB* is involved in the red CPL effect on hypocotyl elongation.

Effect of CPL on biomass production by *Arabidopsis*

Evaluation of the effects of white (red+green+blue) CPL on biomass production by *Arabidopsis*, with biomass is defined as the average fresh weight of an above-ground part of an adult plant, found that the average tissue weights L- and R-CPL were 243 mg and 322 mg, respectively, indicating that white R-CPL produced a 1.26-fold greater biomass than white L-CPL (Figure 3A). To assess the effects of light, *Arabidopsis* was cultured under red, green or blue CPL, although the total fluence of these CPLs differed. The biomasses produced under red (334 mg vs. 285 mg) and blue (74 mg vs. 58 mg) R-CPL were greater than those produced under L-CPL, ratios of 1.17 and 1.27, respectively. In contrast, green CPL had little effect on biomass production, being 198 mg and 199 mg for green L- and R-CPL, respectively (Figure 3B).

UV-Vis absorption spectra of PCB-bound *AtphyB-N651* in *Pr* and *Pfr*

To study the involvement of *phyB* in the observed effects of CPL, UV-visible (UV-Vis) absorption spectra of a PCB-bound sensory module of *Arabidopsis* *phyB*, *AtphyB-N651*, were measured in *Pr* and a photostationary state between *Pr* and *Pfr* induced by saturating with red light illumination (Figure 4A). *Pfr* spectra were constructed by subtracting the *Pr* spectrum from the spectrum of the photostationary state, so that the shoulder on the *Pr* spectrum disappears (Figure 4B). The first absorption peaks of *Pr* and *Pfr* were at 650 nm and 713 nm, respectively, while their second absorption peaks were at 358 and 372 nm, respectively, with the latter having a shoulder at around 415 nm. These absorption peaks are characteristic of those of PCB-

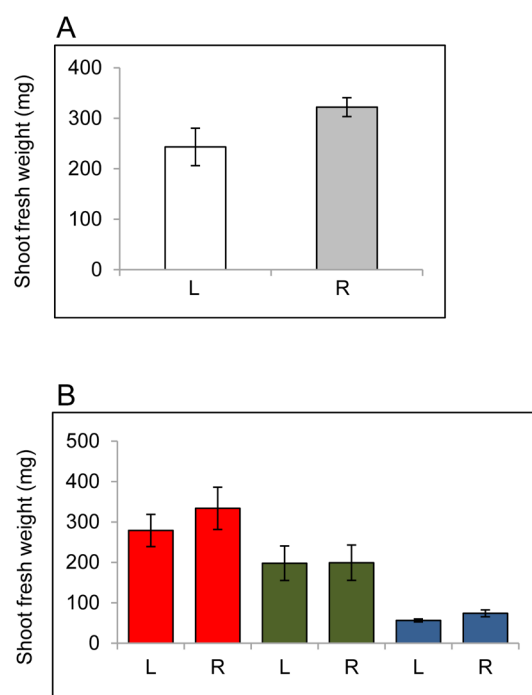


Figure 3. Effect of white CPL (A) and red, green and blue CPL (B) on biomass production by *Arabidopsis*. (A) Seedlings planted in soil were cultured under unpolarized white light for 2 weeks with a 16 h light/8 h dark cycle ($22 \mu\text{mol}/\text{m}^2/\text{s}$) at 22°C . The seedlings were subsequently cultured under white L- (L) or R- (R) CPL with a 16 h light/8 h dark cycle at $10.8 \mu\text{mol}/\text{m}^2/\text{s}$ for 3 weeks at 22°C . Shoots of the adult plants were cut and their fresh weights were measured. $p < 0.07$ by *t*-test, error bar = S.D., $N = 3$. (B) *Arabidopsis* plants were grown under unpolarized white light for 2 weeks, as described in the legend to (A). The plants were subsequently grown under red ($29.7 \mu\text{mol}/\text{m}^2/\text{s}$ for 2 weeks), green ($5.0 \mu\text{mol}/\text{m}^2/\text{s}$ for 3 weeks) and blue ($2.3 \mu\text{mol}/\text{m}^2/\text{s}$ for 3 weeks) L- (L) and R- (R) CPLs, at total fluences of 35.6, 8.1 and 2.8 mol photons, respectively. Shoots of the adult plants were cut and their fresh weights were measured. $p = 0.128, 0.941$ and 0.332 for red, green and blue light, respectively, by *t*-tests, error bar = S.D., $N = 3$.

bound cyanobacteria phytochrome 1 (Cph1) (Hahn et al. 2006) and were about 15 nm blue shifted from those of PΦB-bound *Arabidopsis* *phyB27*, with the blue shift due to the lack of a one π -electron conjugating system at the edge of the linear tetrapyrrole in PCB (Supplementary Figure S1).

CD spectra of PCB-bound *AtphyB-N651* in *Pr* and *Pfr*

CD spectra of PCB-bound *AtphyB-N651* were also measured in *Pr* and a photostationary state between *Pr* and *Pfr* induced by saturating with red light illumination (Supplementary Figure S2). Because of the actinic effect of the strong measuring beam light of CD (see Materials and methods), the *Pr* spectrum during CD measurement showed formation of *Pfr*, as well as a decrease in *Pr* in the photostationary state. The UV-Vis absorption spectra measured immediately after CD measurements (Supplementary Figure S2A) after illumination with saturating far-red and red light were approximated by

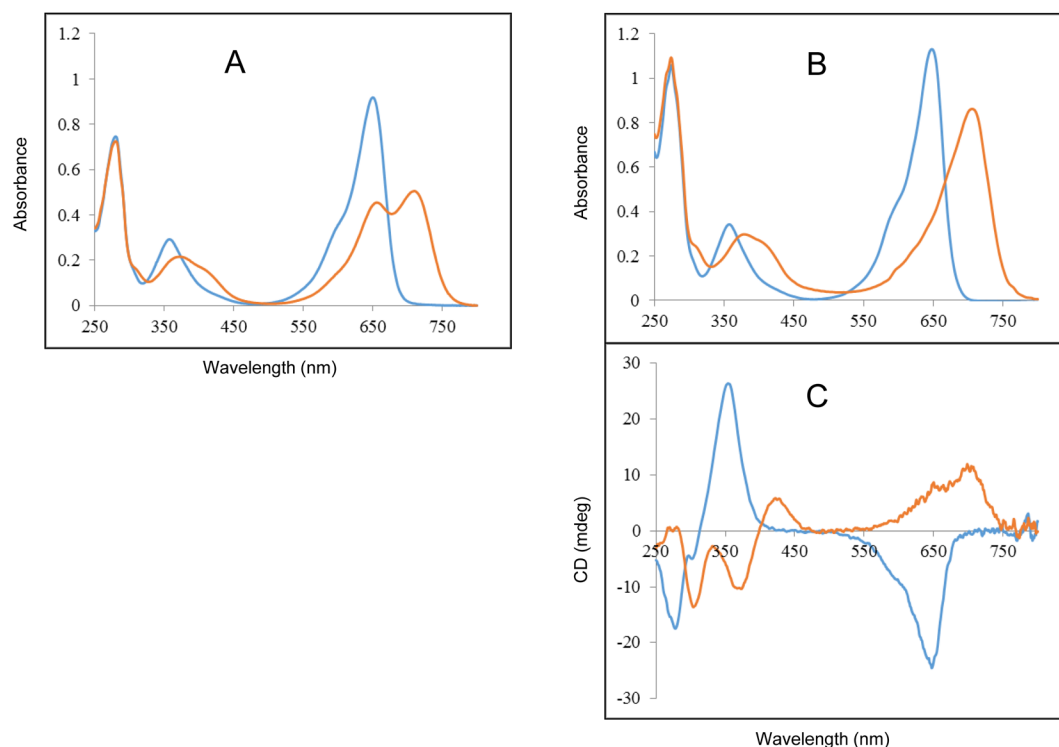


Figure 4. UV-Vis absorption spectra and CD spectra of AtphyB-N651. (A) UV-Vis absorption spectra of PCB-bound AtphyB-N651 in Pr (blue line) and a red light-induced photostationary state (orange line). Spectra of Pr and the red light-induced photostationary state were measured after saturating far-red LPL and under saturating red LPL, respectively, at 25°C. (B, C) UV-Vis absorption (B) and CD (C) spectra of in Pr (blue line) and 100% Pfr (orange line). The absorption spectrum of 100% Pfr was calculated from the absorption spectra of Pr and the red light-induced photostationary state shown in (A). The CD spectra of 100% Pr and 100% Pfr were calculated from the CD spectra of Pr and a red light-induced photostationary state measured at 25°C (Supplementary Figure S2) by correcting for the actinic effects of the light used to measure CD.

superimposition of 89% Pr and 11% Pfr spectra and by 44% Pr and 56% Pfr spectra, respectively (Figure 4B, C). Based on these fractions, the CD (Figure 4C) spectra of 100% Pr and 100% Pfr were constructed from the CD spectra shown in Supplementary Figure S2B. The CD spectrum of Pr has negative and positive CD Cotton effects in the regions of the first and second absorption bands, respectively (blue line in Figure 4C), whereas the Pfr CD spectrum of Pfr has a positive Cotton effect in the region of the first absorption band and complex signals in the region of the second absorption band (orange line in Figure 4B).

Effects of LPL and CPL on the photoreaction of PCB-bound AtphyB-N651

Evaluation of the effects of LPL and CPL on photoreactions from Pr to Pfr (Figure 5) and from Pfr to Pr (Supplementary Figure S3) showed that LPL and both L- and R-CPL induced a reversible phototransformation between Pr and Pfr, similar to that of unpolarized light. These polarizations did not affect the absorption peaks of Pr and Pfr (compare Figure 4A with Figures 5A, B and C and Supplementary Figure S3A–C). The time courses of the photoreactions from Pr to Pfr (Figure 5D and E) and from Pfr to Pr (Supplementary Figure S3D and E) monitored at peaks for Pr (650 nm) and Pfr (715 nm)

fit well with a single exponential curve of a first-order reaction, $\text{Abs}(t) = A \exp(-kt) + B$ where $\text{Abs}(t)$, A , k and B are absorbance at time t , a constant of proportionality, a rate constant and an offset, respectively. Rate constants calculated from the fitting curves are summarized in Table 1. The rate constants for both photoreactions did not differ significantly for L-CPL and R-CPL. In contrast, the rate constants for both photoreactions were slightly higher for LPL than for CPL.

Discussion

Involvement of phyB in the CPL effect on seed germination and hypocotyl elongation

To our knowledge, this study is the first to suggest that L-CPL and R-CPL have different effects on the germination of Arabidopsis and lettuce seeds. Light-induced germination of Arabidopsis seeds has been reported mediated by phyA and phyB, depending on the intensity and duration of light illumination (Shinomura et al. 1996). PhyA mediates seed germination induced by red light of intensity 1–100 nmol/m²/s and far-red light of intensity 0.5–10 μmol/m²/s, both applied after incubation in the dark for 48 h. Red light-induced germination could not be reversed by subsequent far-red light illumination (Shinomura et al. 1996), a phenomenon called the very

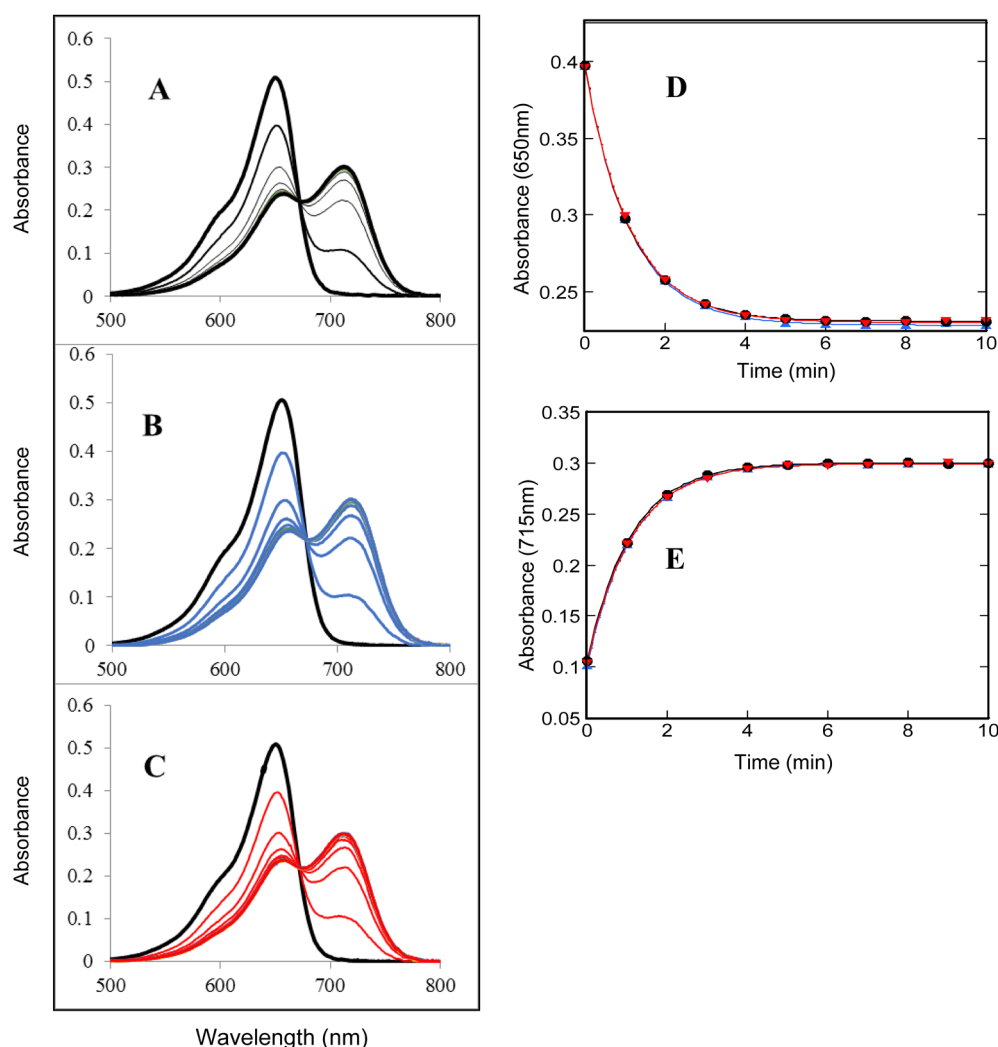


Figure 5. Changes in the UV-Vis absorption spectra of PCB-bound AtphyB-N651 during photoreactive conversion from Pr to a red light-induced photostationary state at 25°C. (A–C) Changes in the spectra of Pr (black thick lines) were monitored by repeat scanning every 1 min (thin lines) for 15 min (thick lines) after the onset of red light illumination of LPL (black lines in A), L-CPL (blue lines in B) and R-CPL (red lines in C). (D, E) Kinetics of photoreactions monitored at Pr (650 nm; D) and Pfr (715 nm; E) peaks. (●), (▲) and (▼) indicate absorbance changes induced by LPL, L-CPL and R-CPL, as determined by the changes in spectra in (A), (B) and (C), respectively. Black, blue and red lines are simulation curves fitted with a single exponential for the first order reaction, as described in the Results.

Table 1. Effect of polarized light on photoreaction rate of PCB-bound AtphyB-N651 at 25°C in a 25 mM Tris-HCl, pH 7.8, buffer containing 0.5 mM Na₂EDTA and 125 mM NaCl.

Reaction	Pr to Pfr			Pfr to Pr		
	LPL	L-CPL	R-CPL	LPL	L-CPL	R-CPL
$K (A_{650})$	0.910	0.887	0.887	0.473	0.467	0.463
$K (A_{715})$	0.915	0.902	0.899	0.476	0.472	0.473

LPL, L-CPL and R-CPL indicate linear, left- and right-handed circularly polarized light respectively. $K (A_{650})$ and $K (A_{715})$ are reaction rates (min^{-1}) calculated from the simulation curves for the time course of the changes in absorbance at 650 nm and 715 nm, respectively, in Figure 5 and Supplementary Figure S3.

low fluence response (VLFR) (Casal *et al.* 2014). In contrast, phyB mediates seed germination induced only by red light of intensity 10–1,000 $\mu\text{mol}/\text{m}^2/\text{s}$ applied after incubation in the dark for 3 h and could be reversed by subsequent illumination with far-red light (Shinomura *et al.* 1996), a phenomenon called the low fluence response (LFR) (Reed *et al.* 1998). Based on the intensity and

timing of the light illumination, germination in the present study corresponds to LFR mediated by phyB. The germination rates of Arabidopsis and lettuce induced by red R-CPL were greater than those induced by L-CPL, indicating that the phyB molecules responsible for the seed germination are able to sense the chirality of red light.

Hypocotyl elongation of wild-type *Arabidopsis* was effectively inhibited under R-CPL than L-CPL. Because this difference was not observed in *phyB*, it was likely due to light reception by *phyB*. Hypocotyl elongation in plant seedlings is inhibited by red light perceived by *phyB* (Reed et al. 1993). The shorter hypocotyl length under R-CPL than under L-CPL was therefore likely due to the *phyB*-mediated photoinhibition of elongation. Shoots of lentils and peas have been shown to grow faster under L- than under R-CPL (Shibayev and Pergolizzi 2011). Moreover, the birefringence of the outer layer of leaves (epidermis) and stems had a negligible effect on light polarization, suggesting that photoreceptors contribute to light perception. Because hypocotyls length was measured in 7-day-old seedlings, the faster growth under L-CPL than under R-CPL may be due to a greater photoinhibition of hypocotyl elongation by R-CPL perceived by *phyB*. All these results (Shibayev and Pergolizzi 2011; Shinomura et al. 1996), as well as our findings, suggest that *phyB* is involved in the differential effects of L- and R-CPL on seed germination and hypocotyl elongation.

Molecular basis of red CPL perception by phyB

Phytochromes have been shown to perceive LPL, with red LPL inducing polarotropism in fern and moss protonemata (Bünning and Etzold 1958). The transition moments of Pr and Pfr in fern protonemata may be aligned in parallel and normally, respectively, to the cell surface at the periphery of the apical hemisphere (Kadota et al. 1985). This may be due to localization of phytochrome molecules on the cell membrane surface, with alignment of their molecular axes and directional changes in the moment of transition during phototransformation from Pr to Pfr (Tokutomi and Mimuro 1989). The phytochrome involved in this polarotropism was found to be neochrome, a kimeric photoreceptor composed of the N-terminal sensory module of phytochrome and full length phototropin (Kawai et al. 2003).

A soluble *phyB* protein, which is present in the cytosol of angiosperms, was shown to be imported into the nucleus upon light activation, forming speckles of as-yet undetermined biological function (Nagatani 2004). Although the orientation of Pfr of *phyB* in the speckles is not known, Pr of *phyB* in the cytosol is not oriented. The different responses to red L-CPL and R-CPL must therefore be due to the molecular nature of *phyB* itself in Pr. The chiroptical spectroscopic properties were therefore evaluated using a PCB-bound sensory module of *AtphyB*, consisting of 651 amino acids residues. Crystallographic studies of Pr have revealed a $5Z_{syn}$, $10Z_{syn}$, $15Z_{anti}$ configuration for the methylene linkers connecting the four pyrrole rings, both for PCB in Cph1 (Essen et al. 2008) and PΦB in *AtphyB*-N90-624 (Burgie

et al. 2014) (Supplementary Figure S1). The differences in the effects of red CPL are therefore due to differences in configurations and conformations of the chromophore in Pr of *phyB*, which is reflected in a CD spectrum. The degree of CD, reported as molar ellipticity θ , can be written as $3300 (\epsilon_L - \epsilon_R)$, where ϵ_L and ϵ_R are the molar absorption coefficients of L-CPL and R-CPL, respectively, and a negative CD signal indicates that ϵ_R is larger than ϵ_L . This is consistent with findings showing that R-CPL generally has greater effects than LCPL. The negative CD signal in the red light-absorbing region may explain, at least in part, the different CPL effects on physiological responses. Upon phototransition from Pr to Pfr, the chromophores of phytochromes isomerize from a $15Z_{anti}$ to a $15E_{anti}$ configuration (Burgie et al. 2014; Ulijasz and Vierstra 2011). These conformational changes result in CD spectral changes similar to the CD spectral changes reported with PCB in Cph1 (Rockwell et al. 2009).

R-CPL is expected to have a larger effect on ϵ , the population of *phyB* molecules photoconverted from Pr to Pfr, than L-CPL. A larger population of Pfr may result in enhanced physiological responses and may explain the enhanced germination and stronger photoinhibition of hypocotyl elongation by R-CPL than by L-CPL. However, the contents of Pfr in the red light-induced photostationary state were almost the same for L- and R-CPL. Furthermore, differences in the reaction rates of phototransformation from Pr to Pfr could not be detected, despite R-CPL likely having a greater reaction rate than L-CPL. This may have been due to the limited sensitivity of our optical measurement systems, with minimal detectable changes in absorbance of 10^{-3} . In contrast, the difference between ϵ_R and ϵ_L was of the order 10^{-6} , as the vertical scales of θ in the CD spectra are in milli-degrees and θ is $3300 (\epsilon_L - \epsilon_R)$. Thus, the different populations of Pfr in the R-induced photostationary state and differences in the reaction rates of L-CPL and R-CPL could not be detected spectrophotometrically.

Possible amplification of the difference in L- and R-CPL signals

Despite the very small differences in CD and undetectable absorption spectroscopy, the present results indicate that *Arabidopsis* can distinguish between R-CPL and L-CPL. Plants as well as animals have various amplification systems for light signals. For example, rhodopsin is highly sensitive and uses well-known biochemical pathways. Carp rhodopsins can induce electrophysiological responses, even when fewer than 1 in 10^5 rhodopsin molecules is photoconverted (Kawamura and Tachibanaki 2008). Plants also have a very highly sensitive response. VLFR can be induced by photoconversion of fewer than 1 in 10^4 *phyA* molecules (Reed et al. 1998), a photoreaction too small to be detected with the spectrophotometer used in the present

study. Although the signaling networks for VLFR and LFR have been described (Xu et al. 2015), the mechanism by which light signals are amplified remains unclear. Known or unknown signal pathways may amplify the small difference in light signals detectable by the CD spectra and undetectable by absorption spectra, resulted in the observed different physiological responses.

Effect of CPL on biomass production

Understanding the effects of CPL on biomass production may provide useful information to increase crop production in plant factories and may help resolve food crises. Biomass differed markedly in adult green *Arabidopsis* plants grown under L- and R-CPL. Many factors control fresh weight of shoots. The growth and development of plants are regulated by environmental light signals received by photoreceptors. Differences in the effects of L- and R-CPL in blue and red light-absorbing regions suggest the involvement of blue light receptors, such as cry or phot, in addition to phy.

Phot is known to increase the biomass of *Arabidopsis*. The fresh weight of wild type *Arabidopsis* was about three times higher than that of the *phot1/phot2* double mutant under red and weak blue light (Takemiya et al. 2005). This difference was likely due to the role of phot in controlling the opening of the stomata (Takemiya et al. 2005) and chloroplast accumulation (Gotoh et al. 2018), which optimize photosynthetic efficiency. Phot has two light, oxygen, and voltage-sensing domains (LOV), LOV1 and LOV2, which bind a flavin mononucleotide (FMN) non-covalently and show a cyclic photoreaction, including transient adduct formation with a nearby cysteine residue (Salomon et al. 2001). Of the two LOV domains, LOV2 play a major role in regulating physiological responses. FMN of LOV2 in the ground state showed a negative CD in the blue light-absorbing region (Corchnoy et al. 2003), indicating that the isoalloxazine ring of FMN exists in an asymmetric environment in protein, compared with a symmetric environment in solution (Abdurachim and Ellis 2006). Taken together, these findings indicate that phot may contribute partly to the larger biomass production under white L-CPL than under white R-CPL.

Phy has been shown to regulate physiological responses in plants, including de-etiolation, shade avoidance and flowering (Franklin and Quail 2010). Cry shows similar regulatory capacity under blue light conditions (Yu et al. 2010). Regulation modes related to biomass production differ depending on the growth stage of plant and the light conditions. For example, phyB and cry1 repress hypocotyls elongation in young plants (Yu et al. 2010), which may reduce the weight of shoots. However, the perception of light by these photoreceptors increased biomass production in adult tissues (Foreman et al. 2011). In its ground (oxidized) form, flavin adenine

dinucleotide (FAD), the chromophore in cry, also showed a negative CD in the blue light-absorbing region (Brazard et al. 2010), but showed little CD in solution (Miles and Urry 1968), similar to FMN of phot. These findings suggest that phyB and cry1 may contribute to the larger biomass production in adult plant under white L-CPL than under white R-CPL.

In addition to light perception by photoreceptors, photosynthesis itself may be involved. L-CPL has shown greater net photosynthesis than R-CPL in a marine alga, *Dunaliella* (McLeod 1957), a finding consistent with the present results on biomass production. However, no concrete evidence to date has shown that L-CPL induces greater photosynthetic activity than R-CPL in higher plants although many studies have used CD (Krausz et al. 2008) or circularly polarized luminescence (Gussakovskiy et al. 2006; Hall et al. 2016), the emission analog of CD, to evaluate the molecular structures and functions of isolated or reconstituted photosynthetic apparatus, such as light-harvesting complexes and reaction centers. These papers reported that the photosynthetic apparatus of these plants was organized chirally, suggesting the need for additional studies to clarify the contribution of photosynthesis to biomass production.

Acknowledgements

We thank Dr. Takeo Sato of Hokkaido University for kind advice about plant germination, hypocotyl elongation and growth and Mr. Hiroshi Kimiada of the JACO Corporation for his kind help adjusting accurate CPL irradiation. This work was supported in part by a Grant-in-aid for Scientific Research on Innovative Areas 22120005 (to S. T.) from MEXT Japan and Grants-in-aid for Exploratory Research 23657105 (to S. T.) and 20651055 (to K. M.) from JSPS, Japan.

Author Contributions

E.L. performed the germination, hypocotyl elongation and growth experiments. K.Z. performed spectroscopic experiments. S.T. supervised the spectroscopic study. T.H., Y.U., and M.I. constructed the CPL irradiation system. H.K. prepared samples for the spectroscopic experiments. J.Y. and K.M. supervised hypocotyl elongation and growth experiments. K.M. conceived the study. E.L., K.Z., S.T., T.H., Y.U., M.I., J.Y. and K.M. discussed the results and their interpretation. E.L., S.T., J.Y. and K.M. wrote the manuscript. All authors have read and approved the final manuscript.

References

- Abdurachim K, Ellis HR (2006) Detection of protein–protein interactions in the alkanesulfonate monooxygenase system from *Escherichia coli*. *J Bacteriol* 188: 8153–8159
- Baar Y, Rosen J, Shashar N (2014) Circular polarization of transmitted light by sapphirinidae copepods. *PLoS One* 9: e86131
- Brady P, Cummings M (2010) Differential response to circularly polarized light by the jewel scarab beetle *Chrysina gloriosa*. *Am Nat* 175: 614–620
- Brazard J, Usman A, Lacombat F, Ley C, Martin MM, Plaza P, Mony

- L, Heijde M, Zabulon G, Bowler C (2010) Spectro-temporal characterization of the photoactivation mechanism of two new oxidized cryptochrome/photolyase photoreceptors. *J Am Chem Soc* 132: 4935–4945
- Bromage TG, Goldman HM, McFarlin SC, Warshaw J, Boyde A, Riggs CM (2003) Circularly polarized light standards for investigations of collagen fiber orientation in bone. *Anat Rec B New Anat* 274: 157–168
- Bünning E, Etzold H (1958) Über die Wirkung von polarisiertem Licht auf keimende Sporen von Pilzen, Moosen und Farnen. *Ber Dtsch Bot Ges* 71: 304–306
- Burgie ES, Bussell AN, Walker JM, Dubiel K, Vierstra RD (2014) Crystal structure of the photosensing module from a red/far-red light-absorbing plant phytochrome. *Proc Natl Acad Sci USA* 111: 10179–10184
- Casal JJ, Candia AN, Sellaro R (2014) Light perception and signalling by phytochrome A. *J Exp Bot* 65: 2835–2845
- Casal JJ, Sanchez RA, Botto JF (1998) Modes of action of phytochromes. *J Exp Bot* 49: 127–138
- Chiou TH, Kleinlogel S, Cronin T, Caldwell R, Loeffler B, Siddiqi A, Goldizen A, Marshall J (2008) Circular polarization vision in a stomatopod crustacean. *Curr Biol* 18: 429–434
- Corchnoy SB, Swartz TE, Lewis JW, Szundi I, Briggs WR, Bogomolni RA (2003) Intramolecular proton transfers and structural changes during the photocycle of the LOV2 domain of phototropin 1. *J Biol Chem* 278: 724–731
- Essen LO, Mailliet J, Hughes J (2008) The structure of a complete phytochrome sensory module in the Pr ground state. *Proc Natl Acad Sci USA* 105: 14709–14714
- Foreman J, Johansson H, Hornitschek P, Josse EM, Fankhauser C, Halliday KJ (2011) Light receptor action is critical for maintaining plant biomass at warm ambient temperatures. *Plant J* 65: 441–452
- Franklin KA, Quail PH (2010) Phytochrome functions in Arabidopsis development. *J Exp Bot* 61: 11–24
- Gagnon YL, Templin RM, How MJ, Marshall NJ (2015) Circularly polarized light as a communication signal in mantis shrimps. *Curr Biol* 25: 3074–3078
- Gotoh E, Suetsugu N, Yamori W, Ishishita K, Kiyabu R, Fukuda M, Higa T, Shirouchi B, Wada M (2018) Chloroplast accumulation response enhances leaf photosynthesis and plant biomass production. *Plant Physiol* 178: 1358–1369
- Gregory RPE, Raps S (1974) The differential scattering of circularly polarized light by chloroplasts and evaluation of their true circular dichroism. *Biochem J* 142: 193–201
- Gussakovskiy EE, Ionov MV, Giller YE, Ratner K, Aripov TF, Shahak Y (2006) Left- and right-handed LHC II macroaggregates revealed by circularly polarized chlorophyll luminescence. *Photosynth Res* 87: 253–265
- Hahn J, Strauss HM, Landgraf FT, Gimenez HF, Lochnit G, Schmieder P, Hughes J (2006) Probing protein–chromophore interactions in Cph1 phytochrome by mutagenesis. *FEBS J* 273: 1415–1429
- Hall J, Renger T, Picorel R, Krausz E (2016) Circularly polarized luminescence spectroscopy reveals low-energy excited states and dynamic localization of vibronic transitions in CP43. *Biochim Biophys Acta* 1857: 115–128
- Harada N, Nakanishi K, Berova N (2012) Electronic CD exciton chirality method: Principles and applications. In: Berova N, Polavarapu PL, Nakanishi K, Woody RW (eds) *Comprehensive Chiroptical Spectroscopy*. John Wiley & Sons, Inc, pp 115–166
- Kadota A, Wada M, Furuya M (1985) Phytochrome-mediated polarotropism of *Adiantum capillus-veneris* L. protonemata as analyzed by microbeam irradiation with polarized light. *Planta* 165: 30–36
- Kawai H, Kanegae T, Christensen S, Kiyosue T, Sato Y, Imaizumi T, Kadota A, Wada M (2003) Responses of ferns to red light are mediated by an unconventional photoreceptor. *Nature* 421: 287–290
- Kawamura S, Tachibanaki S (2008) Rod and cone photoreceptors: Molecular basis of the difference in their physiology. *Comp Biochem Physiol A Mol Integr Physiol* 150: 369–377
- Krausz E, Cox N, Årsköld SP (2008) Spectral characteristics of PS II reaction centres: As isolated preparations and when integral to PS II core complexes. *Photosynth Res* 98: 207–217
- Li J, Li G, Wang H, Wang Deng X (2011) Phytochrome signaling mechanisms. *Arabidopsis Book* 9: e0148
- Li W, Coppens ZJ, Besteiro LV, Wang W, Govorov AO, Valentine J (2015) Circularly polarized light detection with hot electrons in chiral plasmonic metamaterials. *Nat Commun* 6: 8379
- McLeod GC (1957) The effect of circularly polarized light on the photosynthesis and chlorophyll *a* synthesis of certain marine algae. *Limnol Oceanogr* 2: 360–362
- Miles DW, Urry DW (1968) Reciprocal relations and proximity of bases in flavin-adenine dinucleotide. *Biochemistry* 7: 2791–2799
- Mitov M, Dessaud N (2006) Going beyond the reflectance limit of cholesteric liquid crystals. *Nat Mater* 5: 361–364
- Mukougawa K, Kanamoto H, Kobayashi T, Yokota A, Kohchi T (2006) Metabolic engineering to produce phytochromes with phytychromobilin, phycocyanobilin, or phycoerythrobilin chromophore in *Escherichia coli*. *FEBS Lett* 580: 1333–1338
- Nagatani A (2004) Light-regulated nuclear localization of phytochromes. *Curr Opin Plant Biol* 7: 708–711
- Paik I, Huq E (2019) Plant photoreceptors: Multi-functional sensory proteins and their signaling networks. *Semin Cell Dev Biol* 92: 114–121
- Patty CHL, Luo DA, Snik F, Ariese F, Buma WJ, Ten Kate IL, van Spanning RJM, Sparks WB, Germer TA, Garab G, et al. (2018) Imaging linear and circular polarization features in leaves with complete Mueller matrix polarimetry. *Biochim Biophys Acta Gen Subj* 1862: 1350–1363
- Polavarapu PL (2002) Optical Rotation: recent advances in determining the absolute configuration. *Chirality* 14: 768–781
- Reed JW, Elumalai RP, Chory J (1998) Suppressors of an *Arabidopsis thaliana* *phyB* mutation identify genes that control light signaling and hypocotyl elongation. *Genetics* 148: 1295–1310
- Reed JW, Nagpal P, Poole DS, Furuya M, Chory J (1993) Mutations in the gene for the red/far-red light receptor phytochrome B alter cell elongation and physiological responses throughout Arabidopsis development. *Plant Cell* 5: 147–157
- Rockwell NC, Shang L, Martin SS, Lagarias JC (2009) Distinct classes of red/far-red photochemistry within the phytochrome superfamily. *Proc Natl Acad Sci USA* 106: 6123–6127
- Salomon M, Eisenreich W, Dürr H, Schleicher E, Knieb E, Massey V, Rüdiger W, Müller F, Bacher A, Richter G (2001) An optomechanical transducer in the blue light receptor phototropin from *Avena sativa*. *Proc Natl Acad Sci USA* 98: 12357–12361
- Shibayev PC, Pergolizzi RG (2011) The effect of circularly polarized light on the growth of plants. *Int J Bot* 7: 113–117
- Shinomura T, Nagatani A, Hanzawa H, Kubota M, Watanabe M, Furuya M (1996) Action spectra for phytochrome A- and B-specific photoinduction of seed germination in *Arabidopsis thaliana*. *Proc Natl Acad Sci USA* 93: 8129–8133

- Spiesz EM, Kaminsky W, Zysset PK (2011) A quantitative collagen fibers orientation assessment using birefringence measurements: Calibration and application to human osteons. *J Struct Biol* 176: 302–306
- Strout G, Russell SD, Pulsifer DP, Erten S, Lakhtakia A, Lee DW (2013) Silica nanoparticles aid in structural leaf coloration in the Malaysian tropical rainforest understorey herb *Mapania caudata*. *Ann Bot* 112: 1141–1148
- Takemiya A, Inoue S, Doi M, Kinoshita T, Shimazaki K (2005) Phototropins promote plant growth in response to blue light in low light environments. *Plant Cell* 17: 1120–1127
- Tokutomi S, Mimuro M (1989) Orientation of the chromophore transition moment in the 4-leaved shape model for pea phytochrome molecule in the red-light absorbing form and its rotation induced by the phototransformation to the far-red-light absorbing form. *FEBS Lett* 255: 350–353
- Tranter GE (2016) Circular dichroism spectrometers. In: Lindon J, Tranter GE, Koppenaal D (eds) *Encyclopedia of Spectroscopy and Spectrometry*, 3rd Ed. Academic Press, pp 276–293
- Ulijasz AT, Vierstra RD (2011) Phytochrome structure and photochemistry: Recent advances toward a complete molecular picture. *Curr Opin Plant Biol* 14: 498–506
- Vignolini S, Rudall PJ, Rowland AV, Reed A, Moyroud E, Faden RB, Baumberg JJ, Glover BJ, Steiner U (2012) Pointillist structural color in Pollia fruit. *Proc Natl Acad Sci USA* 109: 15712–15715
- Vorlíčková M, Kejnovská I, Bednářová K, Renčíuk D, Kypr J (2012) Circular dichroism spectroscopy of DNA: From duplexes to quadruplexes. *Chirality* 24: 691–698
- Whitmore L, Wallace BA (2008) Protein secondary structure analyses from circular dichroism spectroscopy: Methods and reference databases. *Biopolymers* 89: 392–400
- Xu X, Paik I, Zhu L, Huq E (2015) Illuminating progress in phytochrome-mediated light signaling pathways. *Trends Plant Sci* 20: 641–650
- Yu X, Liu H, Klejnot J, Lin C (2010) The cryptochrome blue light receptors. *Arabidopsis Book* 8: e0135
- Zhuo GY, Lee H, Hsu KJ, Huttunen MJ, Kauranen M, Lin YY, Chu SW (2014) Three-dimensional structural imaging of starch granules by second-harmonic generation circular dichroism. *J Microsc* 253: 183–190